



A Comparison between Virtual Constraint-Based and Model Predictive-Based Limit Cycle Walking Control in Successful Trip Recovery

B. Miripour Fard*

Faculty of Mechanical Engineering, University of Guilan, Rasht, Iran

ABSTRACT: Falling is one of the main causes of the injuries among healthy adults. The foremost causes of the falls are: slipping and tripping. Understanding the phenomenon of human balance recovery against these disturbances is a very important issue in the field of biomechanics as well as in the robotics. Previous studies have shown that human movements can be reproduced using engineering techniques and computational facilities. The prediction of movements can be related to an optimization problem. In the present study, control and prediction of human movements in successful trip recovery are addressed. To formulate the optimization problem, a hybrid dynamic model of the human body with seven degrees of freedom is considered. The tripping perturbation is modeled as an instantaneous contact of the swing leg with an obstacle and the dynamics of impact are derived. Two optimization based methods are used to control and predict the gait: (i) virtual constraint-based limit cycle optimization (ii) model predictive based limit cycle optimization. The simulated results are compared with the human-observed experimental data from the literature. The results show that the second method provides more human-like predictions than the first method in the kinematic level. The second method can predict proper actions to keep away violating constraints in the future. The theoretical results are in agreement with the results of experimental studies on movement adjustments during trip recovery.

Review History:

Received: 3 Jan. 2019
Revised: 8 Jul. 2019
Accepted: 2 Sep. 2019
Available Online: 7 Sep. 2019

Keywords:

Bipedal walking control
Tripping perturbation
Optimization
Model predictive
Virtual constraint.

1- Introduction

Review of biomechanics literature indicates that falling is one of the main causes of the injuries among the healthy adults [1]. The 58 percent of falls occur during walking [2]. The foremost causes of the falls are: slipping (48%) and tripping (25%) [2]. From the perspective of biomechanics researchers, it is very important to understand the phenomenon of balance recovery. On the other hand, although the statistics of human injuries due to fall are not desirable, from the perspective of robotics researchers, the human is still the best walking biped of the planet. It is desirable to produce movements for biped robots in a way that is principally similar to humans' walking behaviors [3]. In recent years, researchers have endeavored to understand the mechanism of falling to develop most robust bipedal robots and technology-based assistive devices for fall prevention. At present, in spite of huge advances, human movement's simulation/prediction is still an open challenge, and there are considerable motivations to understand and imitate human movements in robotics, biomechanics, neuroscience and computer graphics.

The mechanism of tripping recovery has been extensively explored [4-10]. From the experimental studies on recovery from a trip, it is clear that humans adopt three main strategies to prevent falling after a trip

(i). Elevating strategy which consists of elevation of the swing leg to overtake the obstacle. The step is lengthened (longer step time),

(ii). Lowering strategy consists of bringing the foot to the ground as quickly as possible. The step lengths and time are reduced,

(iii). Delayed lowering strategy could be understood as a failed elevating strategy in which the subject first tries an elevating strategy and then switches to a lowering one.

Elevating and lowering strategies are adopted in response to early and late swing perturbations, respectively. Around mid-swing phase of walking, the strategy selection is not mechanically obvious [11]. Potocanac et al. [12] by analyzing leg muscle activity suggested that the initial response to tripping perturbation acts as a "pause," allowing the central nervous system to integrate the necessary information and prepare the subsequent recovery strategy.

Biped robots are designed and fabricated to walk in environments designed for the human. Control of these robots has not yet reached human levels of robustness in standing, walking and running. Walking surfaces irregularities (e. g. protruding nails and boards) or other hazards such as clutter, cords or hoses may cause tripping perturbation. In this circumstances, bipeds should adopt proper responses to avoid falls [13,14]. Trip recovery refers to maintaining biped balance when subjected to a tripping perturbation. This kind of perturbation occurs when the swing foot encounters unexpected obstacles, and an impact takes place. The impact is often characterized by discontinuities in states of the system and a change in the dynamic equations. Generally, control of a system with jumps in the states is very difficult [15]. Consideration of under-actuated models which are

*Corresponding author's email: bmf@guilan.ac.ir



highly efficient and natural looking in comparison with fully actuated bipeds makes it more challenging to study motion planning and control of the system after tripping [16]. The objective of the present paper is to address this problem.

In robotics, many researchers have studied the problem of walking disturbance rejection and stability analysis of biped robots. However, there are still a few types of research on the tripping recovery of biped robots with the aim of reproduction of human-observed movements. In response to tripping and slipping, a reflex controller was designed and tested by Boone and Hodgins [17] to attenuate the effects of the disturbances. Although, they have explored the strategies that enable biped robots to respond to tripping, these strategies were not compared with human-observed strategies. Park et al. [18] designed a finite-state machine that manages changes of controllers for normal walking and a tripping reflex. The transition between the controllers is done based on specially designed contact switches on the end of each leg and the current configuration of the robot. Boer et al. [19] have studied the strategy selection in human trip recovery using simple models and with focusing on the recovery cost minimization. They suggested that the strategy selection for tripping recovery depends on recovery cost, but they did not compare these strategies with real experiments.

Nevertheless, using the mathematical approaches, developed in robotics community, in simulation of various postural tasks such as tripping recovery, will offer opportunities to allow a better comprehension of the human movement formation [20-26]. Furthermore, the results of the current paper and relevant studies by other researchers from biology, biomechanics, and robotics may provide opportunities for joint research projects involving neurobiologists and roboticists.

When the human balance perturbs, he/she executes postural reactions to keep stability and avoid falling. In the biomechanics, one of the fundamental questions is how the brain manages the task of making a decision and performing compensating movements. Many researchers have suggested that the formation of compensating movements can be related to the optimization problem [27]. In the case of formulating the optimization problem, consideration of a cost is necessary. Among the many solutions proposed so far by the robotics community for stable and robust bipedal walking, it seems the following two approaches are more hopeful:

- virtual constraint-based limit cycle generation for biped robots
- model predictive based limit cycle generation for biped robots

These techniques have successfully been implemented in many studies on bipedal walking [28-31]. Although the human balance recovery control is not fully understood yet, we believe that these two approaches in robotics can represent two main hypotheses in biomechanics about neural decision making in response to perturbations. The first hypothesis assumes that neuromuscular control tries to address fundamental functions that are required to capture a specific posture over a step while minimizing energy expenditure. The second approach is based on the leg movement corrections in response to a perturbation to maintain upper extremity in an upright position.

In the current study, a hybrid nonlinear under-actuated biped model with seven degrees of freedom is considered

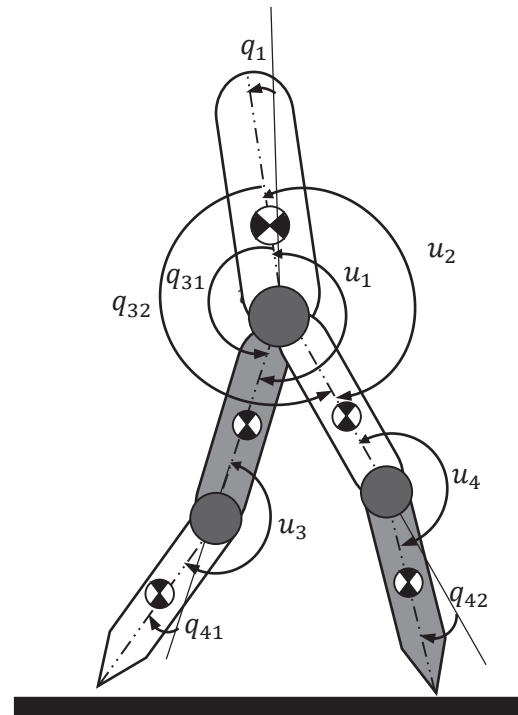


Fig. 1. Model of this study

which experiences a tripping perturbation during walking. The problem of periodic walking pattern generation against tripping perturbation similar to real human reactions is solved using the optimization technique and based on two approaches. Concerning prior works on human movement prediction (predictive dynamics), the contribution of the current work includes implementation of the above-mentioned approaches for trip recovery and comparison with experimental results. The simulation results are compared to the experimental data to inference which theoretical approach is closest to human real postural response.

2- Material and Methods

2- 1- Multibody modeling

The studied bipedal model consists of five rigid segments representing; a torso, two thighs and two shanks (Fig. 1).

The legs end is modeled as a point contact, and there is no torque at the contact point of the legs with the ground. All actuated joints are assumed as frictionless hinges. In all the simulations it is assumed that the friction between the point-foot and the ground is sufficient to prevent sliding. During single support phase, the model has one degree of under-actuation at stance leg contact. It is assumed that the walking surface is rigid and flat and the transition from one leg to another leg (double support) takes place in an infinitesimal length of time. This assumption entails the use of a rigid model to describe the impact of the swing leg with the ground. The dynamic of the model consists of three parts:

- Dynamics during the swing phase (single support phase),
- Dynamics in the double support phase (impact model),
- Dynamics of trip events (impact model).

Single support phase

During the single support phase, the stance leg acts as a pivot, and the model has five degrees of freedom. In this phase the equations of motion are as follows:

$$M(q)\ddot{q} + N(q, \dot{q})\dot{q} + G(q) = Su + F_{ext} \quad (1)$$

In the Eq. (1) q is vector of generalized coordinates ($q = [q_{31}, q_{32}, q_{41}, q_{42}, q_1]$) depicted in Fig. 1, the set (q, \dot{q}) constitutes the state of the biped, $M(q) \in \mathbb{R}^{5 \times 5}$ is the mass-inertia matrix, $N(q) \in \mathbb{R}^{5 \times 5}$ contains the centrifugal and Coriolis forces terms, $G(q) \in \mathbb{R}^5$ is the vector of gravitational forces, $u = [u_1, u_2, u_3, u_4]$ is the vector of control inputs and $S \in \mathbb{R}^{5 \times 4}$ is a torque distribution matrix. The term F_{ext} represents the forces (torques) generated by external interactions.

Double support phase

End of the single support phase is characterized by a collision between the swing foot and the ground. The impact between the end of the swing leg and the ground is modeled as an instantaneous inelastic contact between two rigid bodies. The basic assumptions for impact are

- (i). The impact takes place over an infinitesimally small period of time,
- (ii). The contact of the swing leg with the ground results in no rebound and no slipping of the swing leg and the stance foot naturally lifts from the ground without interaction,
- (iii). Impulsive forces may result in an instantaneous change in the velocities of the generalized coordinates, but the positions remain continuous,
- (iv). The torque supplied by the actuators is not impulsive.

The contact model requires the full seven Degree Of Freedom (DOF) of the robot. The position of the robot in the double support is defined by $q_e = [q, r_0]^T \in \mathbb{R}^7$ where q is the vector of generalized coordinates and $r_0 = [x_0, y_0]$ is the vector of Cartesian coordinates of the stance foot. The velocity of the robot and the acceleration are defined by $\dot{q}_e = [\dot{q}, \dot{r}_0]^T \in \mathbb{R}^7$ and $\ddot{q}_e = [\ddot{q}, \ddot{r}_0]^T \in \mathbb{R}^7$ respectively. The dynamic equation of the model in double support is represented as

$$M_e(q_e)\ddot{q}_e + N_e(q_e, \dot{q}_e)\dot{q}_e + G_e(q_e) + DR = Su + F_g, \quad (2)$$

where $M_e \in \mathbb{R}^{7 \times 7}$ is the symmetric definite positive inertia matrix, $N_e \in \mathbb{R}^{7 \times 7}$ represents the Coriolis and centrifugal forces, $G_e \in \mathbb{R}^7$ is the vector of gravity. D is a matrix that allows taking into account the forces and torques in the dynamic model and R represents the vector of forces exerted on the swing foot by the ground. The term F_g is the vector of the ground reaction forces and torques on the stance foot (there are no torques in this study). The model of impact can be deduced from the integration of Eq. (2) in infinitesimal time as follows

$$M_e(q_e)(\dot{q}_e^+ - \dot{q}_e^-) + DI = D_0 I_0, \quad (3)$$

where I and I_0 are the intensity of Dirac delta-function for the forces exerted by the swing foot and stance foot, respectively. \dot{q}_e^+ is the velocity just after the impact and \dot{q}_e^- is the velocity just before the impact. Since the stance leg is assumed to detach from the ground without interaction, the external forces acting at the pivot point are zero ($I_0 = 0$). Thus, the impact dynamic model is

$$M_e(q_e)(\dot{q}_e^+ - \dot{q}_e^-) = -DI, \quad (4)$$

Additional equations can be obtained from the condition that the impacted leg does not rebound nor slips at impact, which is

$$D^T \dot{q}_e^+ = 0, \quad (5)$$

$$\begin{bmatrix} \dot{q}_e^- \\ \omega_0^- \end{bmatrix} = \begin{bmatrix} 0 \\ 0 \end{bmatrix}, \quad (6)$$

Eqs. (4) to (6) are linear in the unknowns and determine the impulse forces I and the velocity vector of the biped after impact \dot{q}_e^+ . A change of coordinates is also necessary since after impact with ground the swing leg becomes the new stance leg and vice versa. This is done by computation of the orientation and the angular velocity of the swing leg shank. The global impact model that includes velocities just after the impact and the swapping of coordinates can be shortly written as:

$$\begin{pmatrix} q_e^+ \\ \dot{q}_e^+ \end{pmatrix} = \Delta_1(q_e) \begin{pmatrix} q_e^- \\ \dot{q}_e^- \end{pmatrix} \quad (7)$$

where Δ_1 represents the global mapping matrix.

Dynamics of trip events

The tripping perturbation occurs during walking and in the single support phase. The tripping perturbation is characterized by a foot-obstacle impact (Fig. 2(a)). Impact dynamic equations of the model can be derived by applying the principles of linear and angular impulse and momentum. The prior assumptions about double support impact are unchanged except for the type of contact which is assumed to be perfectly elastic in the tripping event. The free-body diagram of the shank (or link i) during impact is shown in Fig. 2(b). The horizontal and vertical components of the impulse to the tip of the leg are p_{iex} and p_{iex} , respectively.

Based on the work of Mu and Wu [32] the impulse and impulse moment equations for the link i (including shank) can be written as

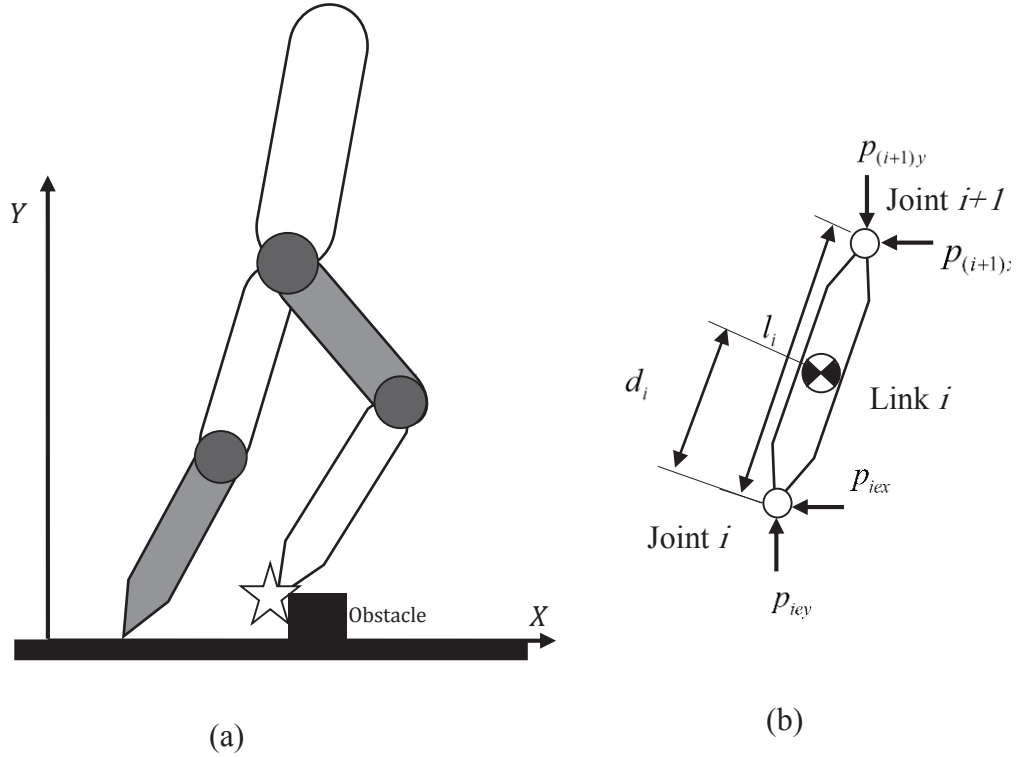


Fig. 2. (a) Schematic view of the model at the instant of tripping perturbation (b) Free body diagram of link i at the instant of tripping impact.

$$\begin{aligned}
 m_i \Delta \dot{x}_{ci} &= \\
 m_i \left[\Delta \dot{x}_1 + \left(\sum_{j=1}^{i-1} a_j l_j \cos(q_j) \Delta \dot{q}_j + d_i \cos(q_i) \Delta \dot{q}_i \right) \right] &= \\
 p_{ix} - p_{(i+1)x} + p_{iex} & \\
 m_i \Delta \dot{y}_{ci} &= \\
 m_i \left[\Delta \dot{y}_1 + \left(\sum_{j=1}^{i-1} a_j l_j \sin(q_j) \Delta \dot{q}_j + d_i \sin(q_i) \Delta \dot{q}_i \right) \right] &= \quad (8) \\
 p_{iy} - p_{(i+1)y} + p_{iey} & \\
 I_i \Delta \dot{q}_i &= p_{(i+1)x} (a_i l_i - d_i) \cos(q_i) \\
 + p_{ix} d_i \cos(q_i) - p_{(i+1)y} (a_i l_i - d_i) \sin(q_i) & \\
 + p_{iy} d_i \sin(q_i), &
 \end{aligned}$$

where m_i , I_i , l_i and d_i , are the mass, inertia, length and center of the mass of the link i. $\Delta \dot{x}_{ci}$ and $\Delta \dot{y}_{ci}$, represent the variation of horizontal and vertical velocities of the center of mass of link i, respectively. $\Delta \dot{x}_1$ and $\Delta \dot{y}_1$ represent the change of horizontal and vertical velocities of the stance shank, respectively. $\Delta \dot{x}_1$ and $\Delta \dot{y}_1$ for the tripping event are zero. a_i is a constant parameter and its value is zero for all the links except for the swing shank in which $a_i \cdot p_{iex}$ and p_{iey} are the horizontal and vertical components of the impulse to the swing shank, respectively.

A set of Eq. (8) is solved to obtain the \dot{q}_i^+ which shows

the velocities just after tripping impact. Here, a change of coordinates is not necessary since after impact with an obstacle the stance and swing legs are not changed. The impact model for the trip which relates the velocities just after impact to velocities just before impact can be presented as follows:

$$\begin{pmatrix} \dot{q}_t^+ \\ \dot{q}_t^+ \end{pmatrix} = \Delta_2(q) \begin{pmatrix} \dot{q}_t^- \\ \dot{q}_t^- \end{pmatrix} \quad (9)$$

$$\Delta_2 = \begin{pmatrix} I_{5 \times 5} & 0 \\ 0 & D_2(q) \end{pmatrix} \quad (10)$$

$D_2(q)$ is obtained by solving the set of Eq. (8) for all links and $I_{5 \times 5}$ is the identity matrix. It is worth noting that there will be an instantaneous jump in the velocities due to tripping perturbation $\dot{q}_t^+ = \Delta_2(q) \dot{q}_t^-$, but the joint positions and coordinates remain continuous and without changes.

Overall model: a hybrid system

The overall model can now be expressed as a hybrid system with impulse effects. Assuming, $x = [q, \dot{q}]^T$ and $u = [u_1, u_2, u_3, u_4]$, in the state space representation the

model can be represented as

$$\left\{ \begin{array}{l} \text{(1) continuous} \left\{ \begin{array}{l} \dot{x} = f(x) + g(x)u, \\ x^- \notin S_i, i = 1, 2 \end{array} \right. \\ \text{(2) Impact model} \left\{ \begin{array}{l} \text{(a) contact with ground} \\ x^+ = \Delta_1(x^-), x^- \in S_1 \\ \text{(b) disturbance} \\ x^+ = \Delta_2(x^-), x^- \in S_2 \end{array} \right. \end{array} \right. \quad (11)$$

where S_i is switching surface. During simulations, contact with the ground is detected when the height of the swing leg is zero and the time in which the tripping perturbation occurs is specified manually.

2- 2- Experimental data

The purpose of this study is to reproduce human reactions in recovery from a tripping perturbation and then to compare the simulation and experimental data. Fortunately, in biomechanics and biological literature there are many experimental studies (e. g. [9, 33-37] for tripping perturbation during walking. Among them, the experimental protocol of the work of Eng et al. [9] is very realistic. Eng et al. [9] have considered a realistic perturbation in which during walking on the ground the swing foot strikes an object. There are some limitations in most of other experimental works on tripping recovery (e.g., consideration of electrical perturbation or a blocking rope attached to the swing foot as a perturbation apparatus, walking on treadmill, etc.). The work of Eng et al. [9] is very close to a real tripping perturbation and we will compare the results with this work. Moreover, the above mentioned work has thorough description about perturbation, kinematics and stepping characteristics. Here, we summarize the procedure was used by Eng et al. [9]:

Ten young healthy male persons (18-29 years) without any histories of neurological and musculoskeletal abnormalities were participated in the study. A thin flexible metal strip on the ground were used as perturbation apparatus. At the moment of perturbation, the strip rotates 90° to an upright position which impose an 8 cm obstruction to the swing foot in early and late swing phase of walking. The instant of contact of swing foot with obstacle were detected using a sensor. The subjects walked along the walkway and the early swing and late swing perturbation were applied. ElectroMyoGraphic (EMG) activity of muscles and kinematics of body segments were recorded during each trials. An elevating strategy of the swing limb in response to the early swing perturbation and a lowering strategy in response to the late swing perturbation were reported by the authors.

2- 3- Optimization

In this section, with the aim of explanation of the generation of the human behavior against tripping perturbation, the optimization problem is formulated based on two approaches:

- Virtual Constraint-based Limit Cycle Optimization

(VCLCO),

- Model Predictive based Limit Cycle Optimization (MPLCO).

These techniques are described as follows.

Virtual constraint-based limit cycle optimization

In this approach, a feedback controller is designed to impose virtual constraints to the dynamics of the model that cause it to walk in a particular stable manner [38]. The virtual constraints depend on joint variables. To implement this approach a set of outputs should be defined as follows:

$$y = h(q) - h^d(s, \beta) \quad (12)$$

In which, s is a monotonically increasing parameter during each step (such as the position of the hip with respect to the stance leg end) and β is design parameter, respectively. h^d represents desired evolution of the controlled variables and is parameterized using the 5th-order Bézier polynomials [38]. β is obtained through an optimization procedure such that the hybrid model (Eq. (11)) will possess an exponentially stable periodic orbit while minimizing the minimum torque cost as follows:

$$J = \int_0^T \|u(t)\|_2 dt \quad (13)$$

where T is the step duration. The optimization problem is subjected to the following constraints:

- Constraint of non-penetration condition,
- Physiological limitation for joint values,
- Limitation on hip height,
- A constraint expressing hip's horizontal and vertical limitations (hip should remain between the feet and above the walking surface)
- A constraint showing that swing leg goes from behind the stance leg to in front of it,
- A friction constraint,
- A constraint on normal ground reaction force.

The above mentioned constraints are extensively used in path planning of biped robots. Adjustments in gait pattern in response to a tripping perturbation can be made by redesigning the virtual constraints. In this paper, the choice of the output function is similar to Plestan et al. [39].

Model predictive based limit cycle optimization

In this approach, the main idea is to choose particular trajectories for the actuated degrees of freedom for which the dynamics of unactuated degrees of freedom of the system tracks the desired trajectory. Trajectories of the actuated degrees of freedom are chosen based on an optimization problem. A feedback controller is then used to track the obtained trajectory and maintain stable periodic walking after tripping. The detail of this approach is given by Chemori and Alamir [29], and we have implemented it for limit cycle walking push recovery of a simple model [30]. A summary of the methodology is described below.

Table 1. Anthropometric parameters of the simulated model

Segment	Shank	Thigh	Torso
Length (cm)	55	47.3	90.7
Mass (kg)	10.1	16.6	56.3
Proximal center of mass position (cm)	33.3	20.5	61.5

By extracting the trunk equation from the dynamic model (Eq. (1)), the expression for the dynamic of the trunk is given as follows:

$$\ddot{q}_1 = f(q_1, \dot{q}_1, \ddot{q}_1, u) \quad (14)$$

where q_1 is the vector of generalized coordinates of lower extremity $q_1 = [q_{31}, q_{32}, q_{41}, q_{42}]^T$. It is assumed that q_1 is completely controllable. Since the closed loop system is obtained by state feedback ($u = f(q, \dot{q}_1^d)$) the Eq. (14) can be written as:

$$\ddot{q}_1 = f(q_1, \dot{q}_1, \ddot{q}_1, q_1^d) \quad (15)$$

In which q_1^d is the reference trajectory of lower extremity which can be parametrized using p parameters. In each decision instant the value of the parameters of the reference trajectories are obtained by solving the following optimization problem:

$$\min_p \left\| q_1 - q_1^{des} \right\|_Q^2 \quad (16)$$

In which q_1^{des} is desired trunk inclination. The reference trajectory is tracked using a feedback controller until next decision instant. In the absence of perturbation, the problem is solved for some desired value of trunk inclination. It should be noted that the optimization problem is subjected to the constraints similar to that of VCLCO.

The optimization problem is solved using a commercial software package (MATLAB release 2014a, The MathWorks, Inc., Natick, MA, USA). MATLAB's constrained optimization function, "fmincon", and event-based Ordinary Differential Equation (ODE) solver are used to solve the nonlinear optimization problem and the set of Eq. (11).

3- Results and Discussion

In this section the comparison of the results is presented. To compare simulation results with real experiments, two simulation scenarios have been considered: (1) early swing perturbation (2) late swing perturbation. These scenarios are addressed by Eng et al. [9] in their experimental study on tripping recovery (section 2. 2). The physical parameters of each segment of the model should be scaled so that the value

of parameters match the experimental subjects. Therefore, for simulation experiments, a 193 cm height and 83 kg weight model similar to the parameters of the reference [9] was considered. The detailed parameters of the model as a fraction of total height and weight were obtained according to anthropometric tables [40]. Table 1 shows the anthropometric parameters of the simulated model. It is assumed that the model walks at a mean velocity of 1.6 ms^{-1} . The optimization and controller parameters are adjusted for all the simulation scenarios. The simulation duration is also chosen sufficient enough to allow complete recovery after perturbation. The sampling time is chosen to be (20 ms).

Fig. 3 shows the phase portrait of the joints in the absence of perturbation. This result has been obtained using VCLCO method and is an illustration of the behavior of the states of the robot. Straight lines show the impacts with the ground. It is seen that there is a periodic orbit for the joints which shows the periodic stability of the motion during normal walking. The similar results are also obtained using MPLCO method. It should be noted that after running simulations based on the VCLCO method, the parameters of the MPLCO method are adjusted to obtain the results very close to the VCLCO method. It is also obvious that in course of several simulations the parameters of the VCLCO method are first tuned to obtain the results very close to Eng et al. [9]. These parameters include: step length, vertical velocity of the tip of the leg just before impact with ground, the desired angle of torso, the desired velocity of hip in horizontal direction just before impact, etc.

Now, the perturbations are imposed to the simulation models to evaluate their capability in prediction of human-observed reactions. The height of obstacle that obstruct the swing leg is 8 cm similar to Eng et al. [9]. In early and late swing perturbations the leg-obstacle momentary impact take place at 20% and 60% of the swing phase, respectively. Comparison between the simulated and experimental results is shown in Figs. 4 to 9. Fig. 4 shows normalized step length during perturbed step of walking in the elevating and lowering strategies observed in response to the early and late swing perturbations, respectively. The normalization is done by dividing the perturbed step length by step length during normal walking. It can be seen that the results of the both methods are in agreement with the experimental data. Both of them predict an increase in the step length in response to the early swing perturbation (elevating strategy) and a decrease in response to the late swing perturbation (lowering strategy). The MPLCO method results in a closer prediction. Fig. 5 shows the corresponding step durations. Both the VCLCO and MPLCO methods predict prolongation of the step time duration for the elevating strategy. These results are in agreement with the experiment. But, unlike the experimental data, VCLCO and MPLCO predict a reduction of the step

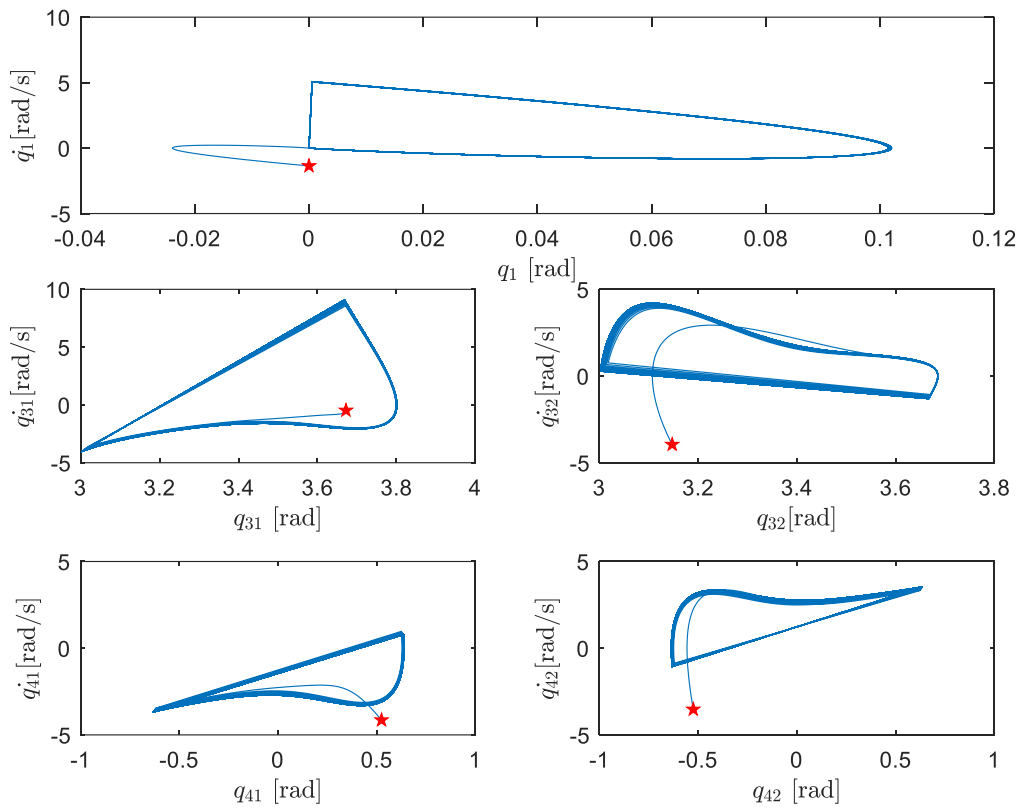


Fig. 3. Phase plane portraits of the joints (generalized coordinates) for normal walking over ten steps. The star dots represent the initial state

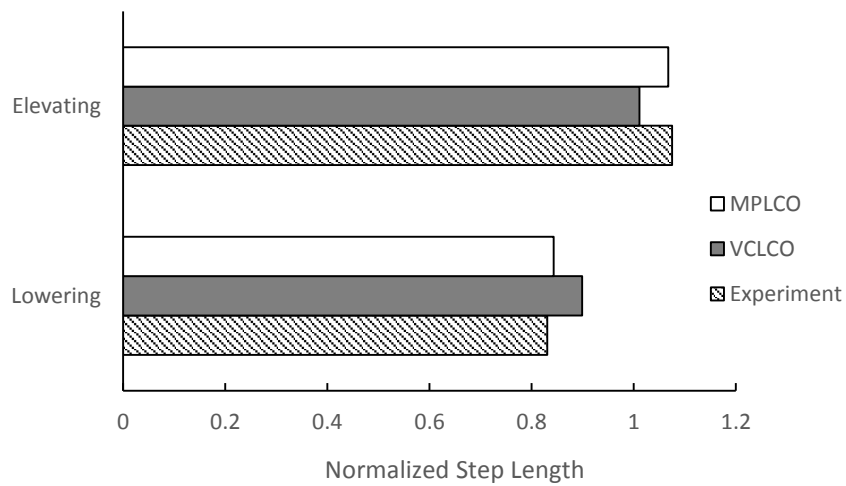


Fig. 4. Comparison of the predicted step lengths for lowering and elevating strategies

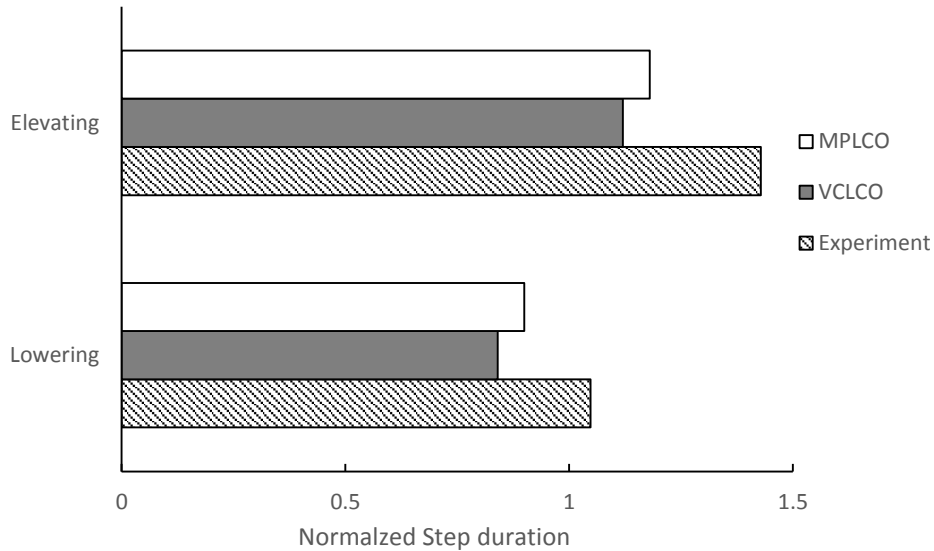


Fig. 5. Comparison of the predicted step duration for lowering and elevating strategies

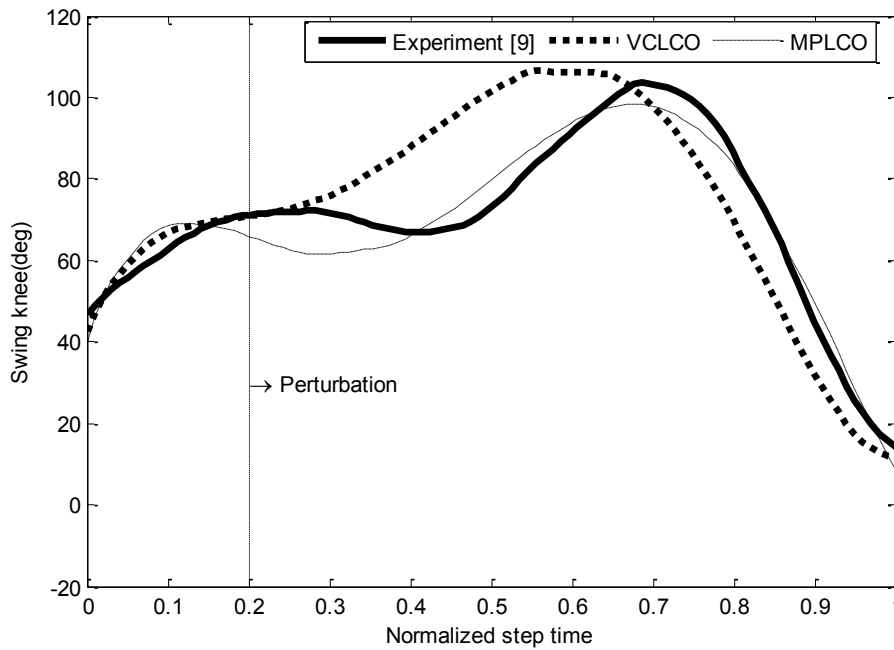


Fig. 6. Comparison of the simulated and experimental angular trajectory of the swing knee joint over the perturbed step in elevating strategy

duration for the lowering strategy. It is possible to adjust the parameters in order to obtain the results which brings the step duration closer to that of the experiment, but this cause the kinematics of the predicted motion to be unnatural. From the Fig. 5 it is apparent that the simulated step duration is shorter than the experimental one. In the other words, the simulated response is faster than the experiment. This is so because of an exact tracking that is achieved using the feedback controller.

Fig. 6 shows the trajectory of the knee joint of the swing foot with respect to normalized step duration in elevating strategy. The simulated angular trajectories of the knee joint for the corresponding model is also shown in Fig. 6.

Fig. 7 shows the trajectory of the hip joint of the swing foot observed in elevating strategy in response to early swing perturbation. The simulated angular trajectories of hip joint for the corresponding model under early swing perturbation is also depicted in Fig. 7. The maximum knee flexion and the terminal value of knee flexion are not close. However, the movement pattern is similar in the mid-swing phase of the response. The prediction of MPLCO method for the knee joint is relatively closer to the actual human movement.

Fig. 8 shows the comparison of the angular trajectory of the knee joint during lowering strategy in response to late swing perturbation (lowering strategy). It is seen that the

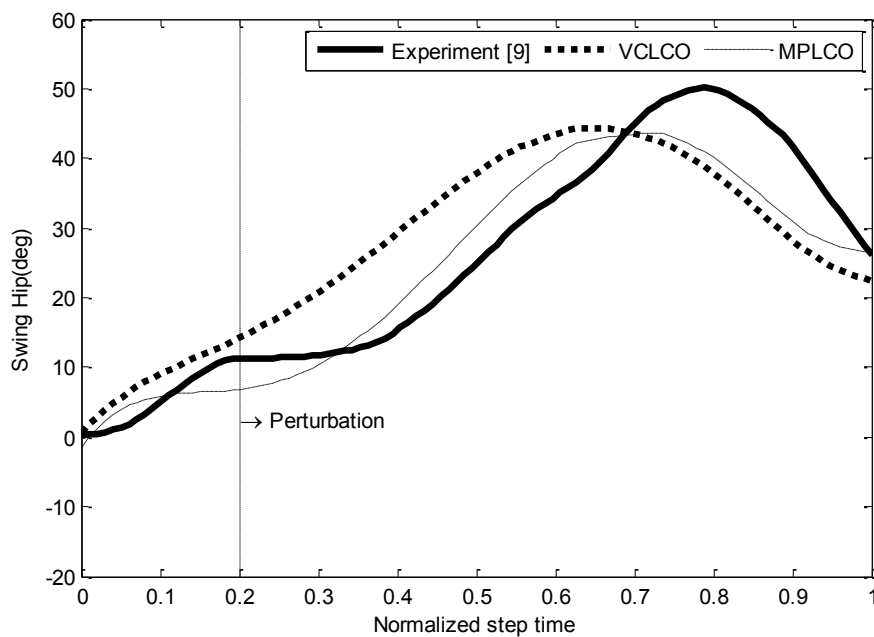


Fig. 7. Comparison of the simulated and experimental angular trajectory of the swing hip joint over the perturbed step in elevating strategy

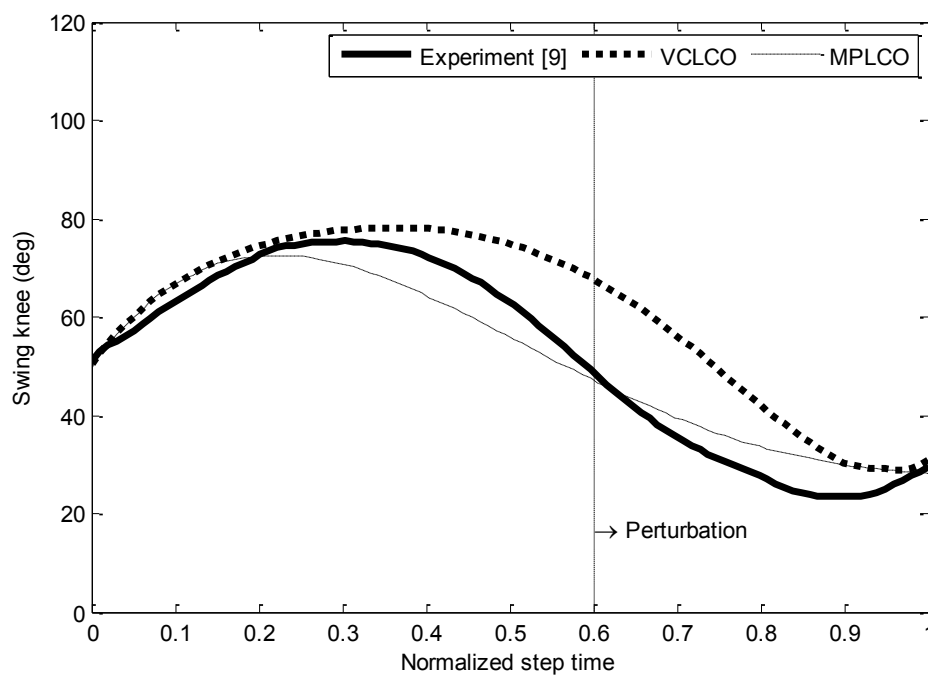


Fig. 8. Comparison of the angular trajectory of the swing knee joint over the perturbed step in lowering strategy

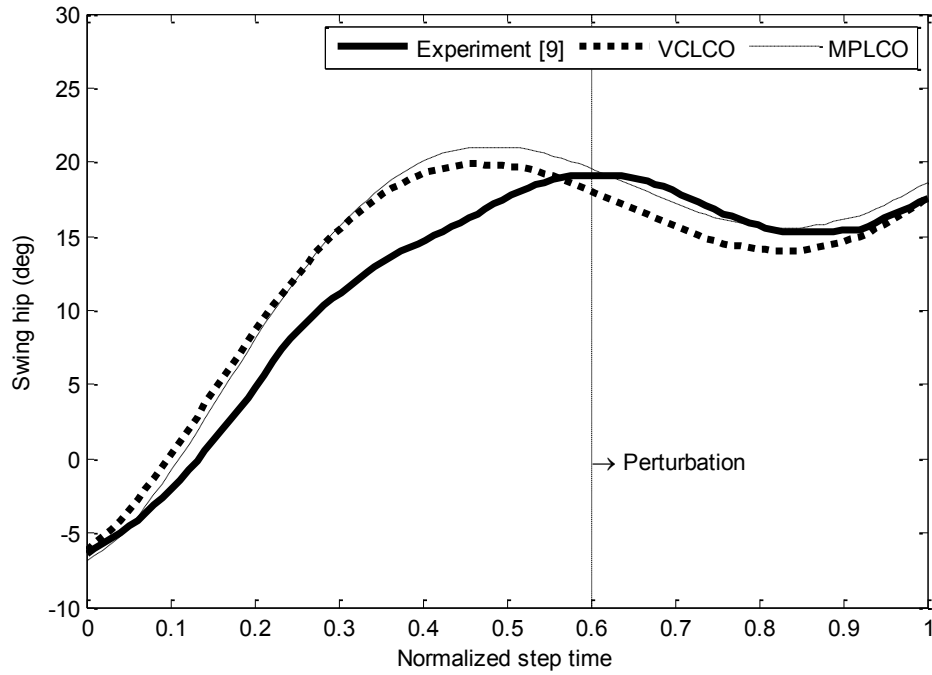


Fig. 9. Comparison of the simulated and experimental angular trajectory of the swing hip joint over the perturbed step in lowering strategy

Table 2. Root mean square error and coefficient of determination (r^2) between experimental joint angle trajectory and simulated results using VCLCO and MPLCO methods

		Elevating		Lowering	
		Knee	Hip	Knee	Hip
VCLCO	RMSE (rad)	13.371	9.689	11.849	4.052
	r^2	0.88	0.81	0.88	0.89
MPLCO	RMSE (rad)	0.926	6.990	5.084	3.508
	r^2	0.99	0.90	0.97	0.94

optimization approaches can predict relatively a similar profile to the experiment for the hip joint. The maximum of simulated hip flexion by VCLCO is more than the other data. The disparity between the result of VCLCO method and experimental results for the hip joint is more than the MPLCO method.

Comparison of the simulated and experimental angular trajectory of the swing hip joint for late swing perturbation is shown in Fig. 9. The VCLCO predicts rather poorly results for the hip joint.

The Root Mean Square Error (RMSE) and correlation (coefficient of determination (r^2)) between experimental and simulation results for the knee and hip joints (depicted in Figs. 6 to 9) are summarized in Table 2. The results show that despite the good correlations between the results the values of the RMSE are not small, especially for the VCLCO method. Generally, the results show that the prediction capability of MPLCO method in kinematic level is more than the VCLCO method.

In the study of limit cycle walkers, quantitative indexes such as the gait sensitive norm [41] is commonly used to measure the robustness of a model against perturbations. However, in the current paper, a direct procedure is used to measure the disturbance rejection abilities of the two theoretical approaches. The maximum obstacle height that can be recovered at the early, mid and the late swing phase of the walking using VCLCO and MPLCO methods have been shown in Fig. 10. As seen, the capability of MPLCO method in tripping recovery at early and mid-swing is more than the VCLCO method, but the robustness of VCLCO method for late swing perturbation is more than the MPLCO method. We reason that in the late swing phase perturbation, the remaining time for leg landing is very short and the MPLCO cannot find a solution for the large perturbations in this short prediction horizon. To the best of the current author's knowledge, there is no experimental work on the tripping rejection of humans against variable height obstacles in the open literature. So, the comparison has only been done between simulated results.

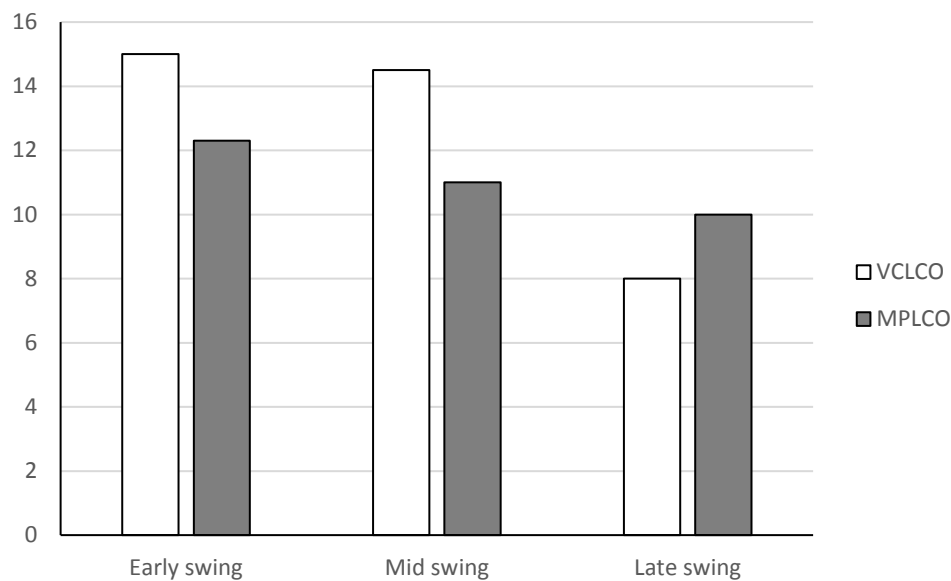


Fig. 10. Maximum obstacle height at early, mid and late swing phase

It is worth noting that human being reactions can be affected by neurological (e.g., muscular activation delay), psychological (e.g., fear of falling) and mechanical limitations (maximum torque and joint ranges of motion). For a mechanical model, only the mechanical limitations make sense. The model of current work, like all the other models based on conventional mechanics and controls, has inherent limitations (e.g., no actuation on the ankle joint, etc.). It should be noted that the comparison has been done just for the perturbed step of walking in which a successful compensation is achieved. It is also worth noting that the balance recovery strategy against tripping may take more steps. Comparison of the subsequent steps was not considered in this study. The lack of comparison in the kinetic level (e.g. comparison of joint torques) is another important limitations of the current work. A reliable method to calculate the joint torques using EMG signals of the human body and a three dimensional high degrees of freedom simulation model should be developed for a comprehensive study in both kinematic and dynamic level.

4- Conclusions

In this paper two optimization based methods have been used to reproduce human reactions under tripping perturbation. To this end, a planar limit cycle model of human body was considered. This kind of model was selected since the motions are achieved by limit cycle walkers are more human-like and natural looking compared with Zero Moment Point (ZMP) based models [16]. The tripping perturbation has been modeled as the contact of the swing leg with an obstacle and the impact equations have been derived. Then, the problem of disturbance rejection was formulated using optimization methods based on VCLCO and MPLCO approaches. The first approach is based on consideration of holonomic constraints on the configuration variables of the model in which initial

and final configurations of the model in a step are considered as design parameters. The second approach is also a trajectory optimization method that considers future actions and constraints. In this approach, the main idea is to choose the particular trajectories for the actuated degrees of freedom for which the dynamics of unactuated degrees of freedom of the system tracks a desired trajectory. The obtained simulation results using the aforementioned approaches, were compared with the results of real experiments on human. Generally, the results of our study clearly showed that the MPLCO method provides remarkably more human-like predictions than the VCLCO method in kinematics level. The success of MPLCO method is mainly owed to the nature of receding horizon control approach in which the optimization is done into the future. This approach can predict proper actions to keep away violating constraints in the future. This may be a reason to conclude that the action of MPLCO approach in tripping recovery is “tripping recovery with thinking about it”. This conclusion is in agreement with the results of Eng et al. [9] and with the results of recent experimental study on movement adjustments during trip recovery by Potocanac et al. [12]. They suggested that a “pause” reaction is initially adopted in response to a tripping perturbation to allow the central nervous system to collect the information and prepare the subsequent movement adjustments.

Nonetheless, further studies should investigate the prediction capability of the theoretical methods in kinetic level to provide more insight into the prediction of human movements in tripping recovery or other perturbations. In future works, the methods will be extended to a musculoskeletal model with higher degrees of freedom and the quality of recovery in kinetic level and energy consumption will also be considered.

References

- [1] Z. Aftab, T. Robert, P.-B. Wieber, Balance recovery prediction with multiple strategies for standing humans, *PloS one*, 11(3) (2016) 1-16.
- [2] M.J.H. Heijnen, S. Rietdyk, Falls in young adults: Perceived causes and environmental factors assessed with a daily online survey, *Human Movement Science*, 46 (2016) 86-95.
- [3] J. Zhang, X. Han, X. Han, Walking quality guaranteed central pattern generator control method, *Proceedings of the Institution of Mechanical Engineers, Part C: Journal of Mechanical Engineering Science*, 228(3) (2014) 569-579.
- [4] Z. Potocanac, J. de Bruin, S. van der Veen, S. Verschueren, J. van Dieën, J. Duysens, M. Pijnappels, Fast online corrections of tripping responses, *Experimental brain research*, 232(11) (2014) 3579-3590.
- [5] T.Y. Wang, T. Bhatt, F. Yang, Y.C. Pai, Adaptive control reduces trip-induced forward gait instability among young adults, *Journal of biomechanics*, 45(7) (2012) 1169-1175.
- [6] M. Pijnappels, M.F. Bobbert, J.H. van Dieën, EMG modulation in anticipation of a possible trip during walking in young and older adults, *Journal of Electromyography and Kinesiology*, 16(2) (2006) 137-143.
- [7] A.F. Cordero, H. Koopman, F.C. van der Helm, Mechanical model of the recovery from stumbling, *Biological Cybernetics*, 91(4) (2004) 212-220.
- [8] A.F. Cordero, M. Ackermann, M. de Lima Freitas, A method to simulate motor control strategies to recover from perturbations: application to a stumble recovery during gait, in: *Engineering in Medicine and Biology Society, EMBC, 2011 Annual International Conference of the IEEE, IEEE, 2011*, pp. 7829-7832.
- [9] J.J. Eng, D.A. Winter, A.E. Patla, Strategies for recovery from a trip in early and late swing during human walking, *Experimental Brain Research*, 102(2) (1994) 339-349.
- [10] A. Murai, K. Yamane, A neuromuscular locomotion controller that realizes human-like responses to unexpected disturbances, in: *Robotics and Automation (ICRA), 2011 IEEE International Conference on, IEEE, 2011*, pp. 1997-2002.
- [11] P. Roos, P. McGuigan, G. Trewartha, Trip recovery strategy selection in younger and older adults and the associated physical demands, in: *33rd Annual American Society of Biomechanics (ASB) Meeting, State College, PA, USA, 2009*.
- [12] Z. Potocanac, M. Pijnappels, S. Verschueren, J. van Dieën, J. Duysens, Two-stage muscle activity responses in decisions about leg movement adjustments during trip recovery, *Journal of neurophysiology*, 115(1) (2016) 143-156.
- [13] O. Kwon, J.H. Park, Reflex control of bipedal locomotion on a slippery surface, *Advanced Robotics*, 16(8) (2002) 721-734.
- [14] B. Miripour Fard, M. Mosadeghzad, Manipulability Based Hierarchical Control of Perturbed Walking, *International Journal of Control, Automation and Systems*, (2019) 1-11.
- [15] M. Mahmoodi, M.K. Manesh, M. Egtesad, M. Farid, S. Movahed, Adaptive passivity-based control of a flexible-joint robot manipulator subject to collision, *Proceedings of the Institution of Mechanical Engineers, Part C: Journal of Mechanical Engineering Science*, 229(5) (2015) 840-849.
- [16] S. Gupta, A. Kumar, A brief review of dynamics and control of underactuated biped robots, *Advanced Robotics*, (2017) 1-17.
- [17] G.N. Boone, J.K. Hodgins, Slipping and tripping reflexes for bipedal robots, *Autonomous robots*, 4(3) (1997) 259-271.
- [18] H.-W. Park, A. Ramezani, J. Grizzle, A finite-state machine for accommodating unexpected large ground-height variations in bipedal robot walking, *IEEE Transactions on Robotics*, 29(2) (2013) 331-345.
- [19] T. de Boer, M. Wisse, F. Van der Helm, Mechanical analysis of the preferred strategy selection in human stumble recovery, *Journal of biomechanical engineering*, 132(7) (2010) 071012.
- [20] T. Buschmann, A. Ewald, A. von Twickel, A. Büschges, Controlling legs for locomotion—Insights from robotics and neurobiology, *Bioinspiration & biomimetics*, 10(4) (2015) 041001.
- [21] L. Martin, V. Cahouët, M. Ferry, F. Fouque, Optimization model predictions for postural coordination modes, *Journal of biomechanics*, 39(1) (2006) 170-176.
- [22] D. Naderi, M. Sadeghi-Mehr, B.M. Fard, Optimization-based dynamic prediction of human postural response under tilting of base of support, *International Journal of Humanoid Robotics*, 9(02) (2012) 1250011.
- [23] D. Naderi, B. Miripour Fard, M. Sadeghi-Mehr, Optimal prediction of human postural response under anterior-posterior platform tilting, *Communications in Nonlinear Science and Numerical Simulation*, 18(1) (2013) 99-108.
- [24] K. An, C. Li, Z. Fang, C. Liu, Efficient walking gait with different speed and step length: Gait strategies discovered by dynamic optimization of a biped model, *Journal of Mechanical Science and Technology*, 31(4) (2017) 1909-1919.
- [25] B. Miripour Fard, A manipulability analysis of human walking, *Journal of biomechanics*, 83 (2019) 157-164.
- [26] B. Miripour Fard, S.M. Bruijn, On the manipulability of swing foot and stability of human locomotion, *Multibody System Dynamics*, 46(2) (2019) 109-125.
- [27] S.J. Hasaneini, C.J.B. Macnab, J.E.A. Bertram, H. Leung, The dynamic optimization approach to locomotion dynamics: human-like gaits from a minimally-constrained biped model, *Advanced Robotics*, 27(11) (2013) 845-859.
- [28] B. Griffin, J. Grizzle, Nonholonomic virtual constraints for dynamic walking, in: *Decision and Control (CDC), 2015 IEEE 54th Annual Conference on, IEEE, 2015*, pp. 4053-4060.
- [29] A. Chemori, M. Alamir, Multi-step limit cycle generation for Rabbit's walking based on a nonlinear low dimensional predictive control scheme, *Mechatronics*, 16(5) (2006) 259-277.

- [30] B. Miripour Fard, A. Bagheri, N. Nariman-Zadeh, Limit cycle walker push recovery based on a receding horizon control scheme, *Proceedings of the Institution of Mechanical Engineers, Part I: Journal of Systems and Control Engineering*, 226(7) (2012) 914-926.
- [31] H. Dai, R. Tedrake, Optimizing robust limit cycles for legged locomotion on unknown terrain, in: *Decision and Control (CDC), 2012 IEEE 51st Annual Conference on*, IEEE, 2012, pp. 1207-1213.
- [32] X. Mu, Q. Wu, On impact dynamics and contact events for biped robots via impact effects, *IEEE Transactions on Systems, Man, and Cybernetics, Part B (Cybernetics)*, 36(6) (2006) 1364-1372.
- [33] M.J. Pavol, T.M. Owings, K.T. Foley, M.D. Grabiner, Mechanisms leading to a fall from an induced trip in healthy older adults, *The Journals of Gerontology Series A: Biological Sciences and Medical Sciences*, 56(7) (2001) M428-M437.
- [34] K. Mitsuoka, Y. Akiyama, Y. Yamada, S. Okamoto, Analysis of Skip Motion as a Recovery Strategy after an Induced Trip, in: *Systems, Man, and Cybernetics (SMC), 2015 IEEE International Conference on*, IEEE, 2015, pp. 911-916.
- [35] C. Shirota, A.M. Simon, T.A. Kuiken, Recovery strategy identification throughout swing phase using kinematic data from the tripped leg, in: *Engineering in Medicine and Biology Society (EMBC), 2014 36th Annual International Conference of the IEEE*, 2014, pp. 6199-6202.
- [36] C. Shirota, A.M. Simon, T.A. Kuiken, Trip recovery strategies following perturbations of variable duration, *Journal of biomechanics*, 47(11) (2014) 2679-2684.
- [37] A.F. Cordero, *Human Gait, Stumble and... fall? Mechanical limitations of the recovery from a stumble*, Universiteit Twente, The Netherlands, 2003.
- [38] E.R. Westervelt, J.W. Grizzle, C. Chevallereau, J.H. Choi, B. Morris, *Feedback control of dynamic bipedal robot locomotion*, CRC press, 2007.
- [39] F. Plestan, J.W. Grizzle, E.R. Westervelt, G. Abba, Stable walking of a 7-DOF biped robot, *IEEE Transactions on Robotics and Automation*, 19(4) (2003) 653-668.
- [40] D.A. Winter, *Biomechanics and motor control of human movement*, John Wiley & Sons, New York, 2009.
- [41] D.G. Hobbelen, M. Wisse, A disturbance rejection measure for limit cycle walkers: The gait sensitivity norm, *IEEE Transactions on robotics*, 23(6) (2007) 1213-1224.

